Investigation of Copper-supported Ceria Nanofibers for Catalytic Oxidation of Diesel Soot

Dan Bahadur Pal
Birla Institute of Technology
Anupama Mishra (anupamamishra.bhu@gmail.com)
University of Petroleum and Energy Studies https://orcid.org/0000-0002-2778-8673

Research Article

Keywords: Ceria, CuO/CeO2, nanofiber, Electrospinning method, Diesel soot emission

Posted Date: March 18th, 2021

DOI: https://doi.org/10.21203/rs.3.rs-295391/v1

Abstract

In the present research, CeO_2 and CuO/CeO_2 nanofibers were synthesized by electrospinning at 12 kV DC by maintaining a tip to collector distance of 10 cm. The morphology of the as-synthesized nanofibers was determined by scanning electron microscopy, and their elemental composition was verified by X-ray photoelectron spectroscopy. The activity of the prepared samples for diesel soot oxidation was determined in a bench-scale fixed bed tubular reactor, and effluent gases were analyzed by online gas chromatography. The variations of working parameters (air flow rate, catalyst-soot ratio, catalyst-soot contact type) were evaluated in a range to optimized reaction conditions for diesel soot oxidation. The catalyst with 40% CuO/CeO_2 had the highest surface area, the smallest crystallite size, and the best activity for diesel soot oxidation (tight contact) at T_f = 318^oC.

1. Introduction

Diesel engines have gained immense popularity as compared to gasoline engines around the world due to their better fuel efficiency, lower operating cost, higher durability, and reliability, and they are the main power source for commercial (trucks, buses, trains, ships) and off-road industrial vehicles (excavation machinery, mining equipment) (Badini et al. 1998). However, a major environmental problem associated with diesel engines is the emission of particulate matter (PM)/soot consisting of carbonaceous soot and a soluble organic fraction (SOF) of hydrocarbons from their exhaust (Abdullah and Bhatia, 2008). Due to the carcinogenic properties of aromatic compounds, photochemical hazardous products of hydrocarbons and black carbon in PM could induce serious health problems and adverse impacts on the environment, such as global warming and climate change (Mishra and Prasad, 2017). Therefore, a possible solution to reduce PM emissions from vehicles is the use of diesel particulate filters (DPFs). The introduction of regenerative catalytic DPFs can reduce soot emission by 98% (Merkel et al. 2001). Among the existing catalytic systems for soot oxidation, noble metal-based catalysts are the most promising ones; however, they are very expensive and sensitive to sulfur poisoning. The key challenge is to find a catalyst that can decrease the combustion temperature of PM from above 600^oC to the range of diesel exhaust (150-450^oC) (Mishra and Prasad, 2014).

Due to the limited availability of noble metals more focus is on the development of non-precious catalysts i.e. CeO_2, NiO, CuO, MoO_3, MnO_2, Co_3O_4, and Fe_3O_4. Among them, copper-ceria catalysts are widely accepted because of their high reducibility at low temperatures. This is due to the synergetic effect between copper and ceria which provides chemically and thermodynamically stable metal oxides (Tang et al. 2014). Wang et al. (2011) reported that nanomaterials have improved catalytic activity than conventional materials due to their higher surface-area-to-volume ratio. Pal et al. (2017) studied Nanostructured Cu-ceria in detail and suggested substantial oxidation ability, specific surface area, and oxygen storage capacity. Moreover, 1-D ceria nanomaterials have a lower agglomeration tendency, possess high porosity, and have an exceptionally high specific surface area. Hence, in recent years, one-

dimensional (1-D) ceria nanomaterials, such as nanorods, nanotubes, nanowires, nanobelts, nanoribbons, nanofibers, have been fabricated for different catalytic applications.

Nanofibers can be synthesized by different methods, such as phase separation, template synthesis, and electrospinning. Among them, electrospinning is considered the most suitable method for nanofiber fabrication. Electrospinning is quite versatile because it produces continuous nanofibers at low cost and permits ease of production and flexibility and better control over fiber diameter, microstructure, and fiber arrangement (Cui et al. 2008).

There is no study reported on Cu-supported ceria nanofiber catalysts synthesized by electrospinning technique for diesel soot oxidation. In the present work we have designed fibrous structured Ceria and Cu-supported ceria catalysts with potentially enhanced trapping and soot oxidation properties. Due to special morphology these nanofibers increases the contact points with the soot particles compared to the layer of catalyst which is conventionally used in diesel particulate filter. In order to correlate the catalytic properties with the structure of nanofibers, the textural and spectral characterization was done. This paper additionally gets picture of the impact of working parameters for example i.e. catalyst-soot ratio, catalyst-soot contact condition, and airflow rate on diesel soot oxidation.

2. Materials And Methods

2.1. Preparation of Catalysts

Cerium nitrate hexahydrate ($Ce(NO_3)_3.6H_2O$; Sigma-Aldrich) and cupric acetate monohydrate ($Cu(CH_3COO)_2.H_2O$; SDFCL) precursors were used as received. Polyvinyl pyrrolidone (PVP; Sigma-Aldrich) was used as the base polymer because of its large molecular weight and high solubility in polar solvents. Ethanol (Merck) and de-ionized water were selected as the solvent and the co-solvent, respectively. Aqueous solutions with 0 mol%, 20 mol%, 40 mol%, and 60 mol% of Cu were prepared by dissolving appropriate amounts of $Cu(CH_3COO)_2.H_2O$ in a solution of 0.4 g of cerium nitrate hexahydrate and 4 mL of de-ionized water kept in five different vials. In another set of four vials, 10% (w/v) PVP solutions were prepared by adding an appropriate amount of PVP in 8 mL of ethanol followed by magnetic stirring. In order to prepare spinning solutions, the contents of the first set of four vials were added separately to the vials containing PVP-ethanol solutions. The contents of the vials were mixed, and acetic acid was added drop-wise (2–3 drops) to each vial. The as-mixed solutions were then magnetically stirred for three hours at room temperature to obtain homogeneous solutions.

Each precursor solution was drawn in a plastic syringe (6 mL) equipped with a stainless-steel flat-tip needle (21 gauges). The syringe was mounted vertically and attached to a syringe pump. The flow rate from the syringe was set at 1 mL/h. A metallic collector plate covered with an aluminum foil was kept directly under the needle tip to collect nanofibers. The distance between the syringe tip and the collector plate was maintained at 10 cm. The syringe, the stainless-steel needle, and the solution delivery tube were

washed with ethanol before casting fibers from a new solution. The as-prepared nanofibers were aged under ambient conditions for 24 h and then calcined in the stagnant air at 500^{o}C for three hours.

2.2. Preparation of Diesel Soot

The real soot was prepared by the partial combustion of locally available commercial diesel (HP) in a lamp with limited air supply and collected on the inner walls of an inverted beaker kept over the lamp. The soot was then collected from the recipient walls of the beaker and dried in an oven overnight at 120^{o}C to remove moisture and volatile components. The dried soot was stored in an air-tight bottle for future experiments.

2.3. Characterization of Catalysts

The textural characterization of the catalysts was carried out in a Micromeritics ASAP 2020 analyzer based on the low-temperature N_2 physisorption method. The phase compositions of the catalysts were identified by a powder X-ray diffraction diffractometer (XRD; Rigaku Ultima IV) under Cu-Kα1 radiation (λ = 1.5405 Å) with a nickel filter operating at 40 mA and 40 kV. The Fourier-transform infrared (FTIR) spectra of the catalysts were recorded in the range of 400–4000 cm^{-1} by a Shimadzu 8400 FTIR spectrometer equipped with KBr pellets at room temperature. The scanning electron micrographs (SEM) of the catalysts were recorded by a Zeiss EVO 18 SEM under an accelerating voltage of 15 kV and a magnification of 1000X. The surface compositions and chemical states of constituent elements in the catalysts were determined by X-ray photoelectron spectroscopy (XPS) in an Amicus Kratos analytical unit under Mg-Ka X-ray radiation at15 kV and 12 mA. The binding energy scale was calibrated by setting the main C 1s line of adventitious impurities at 284.7 eV, leading to uncertainty of ± 0.2 eV in peak positions.

2.4. Activity measurement of the Catalysts

The performances of the as-prepared catalysts for diesel soot oxidation were evaluated in a compact fixed bed tubular quartz reactor. The reactor consisted of two co-axial glass tubes with 20 mm and 50 mm diameters. A helical coil of quartz tube existing between the co-axial tubes served as a pre-heater of the air. A hole was present in the lower part of the outer tube to prevent breakage due to the expansion or contraction of air between the co-axial tubes. The pre-heated air entered the catalyst bed and flowed to the inner tube. The product stream from the bottom of the reactor was cooled to ambient temperature in a condenser and then analyzed by online gas chromatography.

The reactor was mounted vertically in a split open furnace. The down airflow stream was used to avoid the distortion of the catalyst bed. The soot catalyst (catalyst bed diameter and height were 20 mm and 1.27 mm, respectively) was placed on a thin layer of quartz wool, which was supported on a perforated quartz disc inside the inner tube. A thermocouple well consisting of a 4 mm diameter tube was inserted axially from the bottom to the center of the disc for temperature measurement and control. In order to evaluate the catalytic activities of the catalysts, 110 mg of each catalyst-soot mixture was placed in the reactor and then oxidized till the total conversion of the soot at a constant heating rate of 1 ^{o}C.min^{-1}. Before the reactions, each soot-catalyst mixture with a weight ratio of 1:10 was milled in an agate mortar

for tight contact and with a spatula for loose contact. The detailed method of soot conversion calculations by gas chromatography is explained in the literature (Mishra and Prasad, 2015). Tight contact condition was used to explore the intrinsic activity of the catalysts because soot and catalysts were ground together to produce more contact points while loose contact mode was used to simulate real soot- catalyst contact inside catalytic converter (Bueno-López et al. 2007).

3. Result And Discussion

3.1. Textural characterization of catalysts by N_2-sorption

The textural properties of the ceria nanofibers (BET surface area, total pore volume, and average pore diameter) are summarized in Table 1. It is noticeable that the ceria nanofibers had a high specific surface area of 80–102 $m^2.g^{-1}$ and an average pore diameter of 108–130 Å. In comparison to pure ceria, the surface area of the Cu-supported Ceria nanofibers increased gradually when 10 wt%, 20 wt%, and 40 wt% of copper oxide were added. However, a drop in the surface area was observed at the highest copper oxide loading content of 60 wt%. The incorporation of 10–40wt% of CuO favored the increase in porosity, causing an increase in the surface area from 80 $m^2.g^{-1}$ to 102 $m^2.g^{-1}$. In contrast, the incorporation of 60 wt% CuO decreased the porosity and widened the pore distribution, causing the blocking of pores and a drastic decrease of the surface area to 93 $m^2.g^{-1}$.

Table 1
Textural characterization of Ceria nanofibers catalysts

Catalyst	Textural Characteristics			
	S_{BET} (m^2 g^{-1})	Avg Pore dia. (Å)	Total Pore Volume (cm^3 g^{-1})	Crystallite Size (nm)
CeO_2	80	130	0.12	14
20% Cu-CeO_2	90	117	0.16	11
40% Cu-CeO_2	102	108	0.36	9
60% Cu-CeO_2	93	115	0.14	12

3.2. XRD Analysis of the Catalysts

The XRD patterns of the CeO_2 and CuO/CeO_2 nanofibers with different copper loadings (20–60 mol%) are illustrated in Fig. 1. The detected characteristic peaks correspond to the crystalline planes of pure cubic cerium oxide (ceria fluorite structure; JCPDS 34–0394). The small difference in the widths of these ceria peaks indicates different ceria domain sizes. Moreover, in the Cu-supported catalysts, the reflections of

CuO (copper oxide; JCPDS: 45–0937) were prominent at 33.8º and 56.67º. The most intense reflection of CeO_2 was detected at 2θ = 28.83º. The average crystallite size of CeO_2 (14 nm) and CuO/CeO_2 (9–12 nm) were calculated by the Debye- Scherer formula (Table 1). The intensity of the CuO peaks increased with the rising copper loading in the catalysts; however, no significant difference was observed between the pure and Cu-loaded ceria nanofiber catalysts. It is already reported that Cu impregnation marginally influences the lattice parameters of ceria. When the fluorite-like lattice of ceria was doped with divalent Cu2þ cations, the small ionic radii of both Cu and Cu2þ caused a decrease in lattice parameters; however, the increased vacancies and lattice distortion led to an increase in lattice parameters (Si et al. 2012).

3.3. FTIR Characterization

The FTIR spectra of the CeO_2 and CuO/CeO_2 nanofibers are displayed in Fig. 2. Broad bands at 3700–3000 cm^{-1} appeared due to the stretching vibration of the hydroxyl (OH) group of chemisorbed water. The significant enhancement in the absorption band at 500–1060 cm^{-1} confirms the formation of CeO_2 nanofibers. Some authors (Liu et al. 2008; Girija et al. 2011) have assigned stretches above 1200 cm^{-1} to O-H bonds of residual water and C-C and C-H bonds of residual polymer and stretches below 1200 cm^{-1} to Ce-O bonds. In the present experiment, the bands around 3440 cm^{-1}, 1630 cm^{-1}, 1385 cm^{-1}, and several stretches below 1200 cm^{-1} confirm that the samples contained copper acetate and cerium nitrate (used as precursor).

3.4. SEM Characterization

The SEM analysis confirmed the formation of cylindrical nanofibers with varying diameters. Figure 3 exhibits the SEM images of the pure and Cu-supported ceria nanofibers with varying copper loadings (0–60 mol%). The average diameters of the ceria nanofibers containing 20 mol%, 40 mol%, and 60 mol% of Cu were measured as 117 nm, 108 nm, and 115 nm, respectively. Tang et al. (2012) has been prepared Pt/CeO_2 nanofibers by electrospinning method and reported the average diameter of nanofibers ranged from 80 to 120 nm. Jayakumar et al. (2017) also reported the CeO_2 nanoparticles prepared with large size have sphere like structure with average particle size of 110 nm. Shan Xu and others reported an average diameter of green nanofiber as around 200nm (Xu et al. 2011). The reduction in diameter takes place due to the loss of PVP and other organic compounds during calcination (Fox et al. 2008).

3.5. X-Ray Photoelectron Spectroscopy (XPS)

The XPS spectra of the pure and Cu-supported CeO_2 nanofibers calcined in the air at 500ºC are exhibited in Fig. 4. The $Ce3d_{5/2}$ and O1s spectra existed in the binding energy (BE) range of 880–882 eV and 529–530 eV, respectively. The Cu $2p_{3/2}$ spectrum was difficult to interpret due to the overlapping peaks of different Cu species in the BE range of 932–933 eV. (Fox et al. 2008) have discussed the presence of overlapping CuO and Cu_2O peaks in this range and the dynamic behavior and mobility of Cu_2O, CuO, and

$Cu^{x+}Ce$ due to oxidative/reductive conditions. Therefore, the XPS analysis of Cu must be considered in conjunction with other characterization methods to elucidate the nature of Cu ions in these catalysts (Gibbons et al. 2014). The rise in the relative strength can be ascribed to the incorporation of CuO into the ceria lattice during oxidation at high temperatures.

3.6. Soot Oxidation over Ceria nanofibers

A soot oxidation reaction is a typical heterogeneous catalytic reaction in which solid particles act as reactants. The catalytic activities of the nanofibers were measured at the temperatures at which 0%, 50%, and 100% of weight loss were detected (denoted as T_o, T_{50}, and T_f, respectively). The soot conversion percentages for different catalysts under the loose and tight contacts are presented in Fig. 5. The T_o, T_{50}, and T_f values of the catalysts are reported in Table 2. The T_o, T_{50}, and T_f values of the 40% Cu-CeO_2 catalyst were measured as 258°C, 305°C, and 370°C, which are lower than those of the pure and Cu-supported CeO_2 catalysts (Table 2 and Fig. 5), indicating that the 40% Cu-CeO_2 catalyst had much higher soot combustion activity under the loose contact. The catalytic activity was improved under the loose contact in the order of 40% Cu-CeO_2 > 60% Cu-CeO_2 > 20% Cu-CeO_2 > CeO_2. Generally, a mechanical force generates tight contact between diesel soot and a catalyst. Under the tight contact, the 40% Cu-CeO_2 catalyst exhibited the highest catalytic activity for soot oxidation and resulted in the lowest T_o, T_{50}, and T_f values of 201°C, 246°C, and 318°C, respectively (Table 2). In addition, the T_m (temperature at the maximum soot combustion rate) values of the Cu-supported CeO_2 nanofibers were compared with those of previously reported CeO_2 catalysts (Aneggi et al. 2014; Miceli et al. 2014). The T_m of the 40% Cu-CeO_2 catalyst was found as 267^oC, which is much lower than those of other catalysts (above 400^oC). Therefore, the 40% Cu-CeO_2 catalyst possessed an obvious advantage with a much lower T_{50} value under the tight contact. The as-prepared Cu-supported ceria nanofibers with different Cu percentages exhibited different activities for soot combustion under the loose and tight contacts. The oxidation of diesel soot is directly dependant on three factors. The first one is the reducibility of the transition metal cations in order to produce oxygen vacancies. These vacancies are essential to allow the soot oxidation. The second factor is the amount of -oxygen available to initiate the reaction of soot oxidation into CO_2. The third factor is crystallite size and surface area.The 40% Cu-CeO_2 catalyst has high specific surface area and consecutively increased activity of the catalyst. The observation is obvious as the catalysis is a surface phenomenon, higher the surface contacts (tight contact) higher the activity. Other side is that oxygen vacancy order to disorder transition occurs when temperature increases which can decrease the mobility of oxygen species in the bulk and result in the decreasing soot oxidation over 60% Cu-CeO_2. In order to verify the reproducibility of the experimental data, each experiment was performed at least twice for soot oxidation, and the data were found to be reproducible with ± 1% of deviation.

Table 2
Characteristic light off temperature for soot oxidation over Ceria nanofiber catalysts

Catalyst (nanofibres)	Loose Contact			Tight Contact		
	T_o(°C)	T_{50}(°C)	T_f(°C)	T_o(°C)	T_{50}(°C)	T_f(°C)
CeO_2	312	387	451	263	330	378
20% Cu-CeO_2	227	340	423	210	289	361
40% Cu-CeO_2	258	305	370	201	246	318
60% Cu-CeO_2	299	352	403	231	289	358

Table 3
(a). Characteristic light off temperature of soot oxidation over 40% Cu-CeO_2 catalyst for with different Catalyst/soot ratio

Catalyst/Soot Ratio	T_o(°C)	T_{50}(°C)	T_f(°C)
05:1	251	299	368
10:1	201	246	318
15:1	218	270	334
20:1	232	283	345

Table 3
(b). Characteristic temperature of soot oxidation over 40% Cu-CeO_2 at different space velocities

GHSV (h^{-1})	T_i(°C)	T_{50}(°C)	T_f(°C)
7500	230	264	335
15000	224	257	326
22500	201	246	318
30000	256	279	341

The catalyst-soot ratio and gas hourly space velocity (GHSV) for soot oxidation on the 40% Cu-CeO_2 catalyst were further optimized. The activity orders at different catalyst-soot ratios were found in the following descending sequence 10:1 > 15:1 > 20:1 > 5:1 (Fig. 6 and Table 3 (a)). The increasing GHSV from 7500 h^{-1} to 22500 h^{-1} caused a decrease in the characteristic temperatures (T_i, T_{50}, T_f); however,

the further rise in the flow rate to 30000 h^{-1} increased the characteristic temperatures (Fig. 7). This phenomenon explains two counter effects of the increasing GHSV on soot oxidation. The increasing airflow rate generated more oxidants (O_2) and improved the combustion of soot particles. Further, the increase in the airflow rate shortened the contact time of the reactants and negatively affected soot oxidation. These two counter effects resulted in the optimum GHSV value of 22500 h^{-1} at the lowest characteristic temperatures of T_i = 201^oC, T_{50} = 246^oC, and T_f = 318^oC. Table 3(b) presents the characteristic temperatures for soot oxidation at different GHSV values.

4. Conclusions

Four catalysts, pure CeO_2 and Cu-supported CeO_2 nanofibers containing 20 mol%, 40 mol%, and 60 mol% Cu were successfully fabricated by electrospinning. The average diameter of the pure CeO_2 nanofibers was larger than that of the Cu-loaded CeO_2 ones due to the reduction of the gel solution viscosity after the addition of copper acetate monohydrate. Moreover, the average diameter of the nanofibers decreased by about 20–30% after calcination. The optimum catalyst composition for diesel soot oxidation after calcination in the air was 40% Cu-CeO_2 (T_f = 318^oC and 370^oC for tight and loose contacts, respectively). The high catalytic activity of the 40% Cu-CeO_2 nanofibers could be elucidated from the following aspects: first, the nanoscale size of both the catalyst and soot particulates ensured a high contact efficiency between them, and second, the synergistic effect of Cu and CeO_2 increased the oxidation ability of the catalyst.

Declarations

Acknowledgements

The authors thankfully acknowledge Indian Institute of Technology (BHU), Varanasi, for laboratory facility, and the financial support from MHRD, Govt. of India. One of the authors, Anupama Mishra is thankful to the SEED Grant issued by the University of Petroleum and Energy Studies, Dehradun, India.

References

1. Abdullah AZ, Bhatia S (2008) Improvement of loose contact diesel soot oxidation by synergic effects between metal oxides in K_2O-V_2O_5/ZSM-5 catalysts. Catal Commun 9:1196–1200. https://doi.org/10.1016/j.catcom.2007.11.003
2. Aneggi E, Wiater D, Leitenburg C, Llorca J, Trovarelli A (2014) Shape-Dependent Activity of Ceria in Soot Combustion. ACS Catal 4:172–181. https://doi.org/10.1021/cs400850r
3. Badini C, Saracco G, Serra V, Specchia V (1998) Suitability of some promising soot combustion catalysts for application in diesel exhaust treatment. Appl Catal B: Environ 18:137–150. https://doi.org/10.1016/S0926-3373(98)00038-1

4. Bueno-López A, Krishna K, van der Linden B, Mul G, Moulijn JA, Makkee M (2007) On the mechanism of model diesel soot-O_2 reaction catalysed by Pt-containing La^{3+}-doped CeO_2: A TAP study with isotopic O. $_2$Catal Today 121:237–245. https://doi.org/10.1016/j.cattod.2006.06.048
5. Cui Q, Dong X, Wang J, Li M (2008) Direct fabrication of cerium oxide hollow nanofibers by electrospinning. J Rare Earths 26:664–669. https://doi.org/10.1016/S1002-0721(08)60158-1
6. Fox EB, Lee AF, Wilson K, Song C (2008) In-situ XPS Study on the Reducibility of Pd-Promoted Cu/CeO_2 Catalysts for the Oxygen-assisted Water-gas-shift Reaction. Topics in Catal 49:89–96. https://doi.org/10.1007/s11244-008-9063-6
7. Gibbons WT, Liu TH, Gaskell KJ, Jackson GS (2014) Characterization of palladium/copper/ceria electrospun fibers for water–gas shift catalysis. Appl Catal B: Environ 160–161:465–479. https://doi.org/10.1016/j.apcatb.2014.06.001
8. Girija D, Naik HSB, Sudhamani CN, Kumar BV (2011) Cerium oxide nanoparticles - a green, reusable, and highly efficient heterogeneous catalyst for the synthesis of Polyhydroquinolines under solvent-free conditions. Archives of Appl Sci Res 3:373–382. http://scholarsresearchlibrary.com/archive.html
9. Jayakumar G, Irudayaraj AA, Raj AD (2017) Particle Size Effect on the Properties of Cerium Oxide (CeO_2) Nanoparticles Synthesized by Hydrothermal Method. Mechanics, Materials Science & Engineering, Magnolithe, 2017, 9 (1).Doi ff10.2412/mmse.3.4.481ff. ffhal-01499374
10. Liu Z, Chen J, Zhou R (2008) Influence of Ethanol Washing in Precursor on CuO-CeO_2 Catalysts in Preferential Oxidation of CO in Excess Hydrogen. Catal Lett 123:102–106. https://doi.org/10.1007/s10562-008-9401-0
11. Merkel GA, Beall DM, Hickman DL, Vernacotola MJ (2001) Effects of Microstructure and Cell Geometry on Performance of Cordierite Diesel Particulate Filters. SAE paper, 01-0193. https://doi.org/10.4271/2001-01-0193
12. Miceli P, Bensaid S, Russo N. Fino D (2014) CeO_2-based catalysts with engineered morphologies for soot oxidation to enhance soot-catalyst contact. Nanoscale Res Letts 9:254–264. 10.1186/1556-276X-9-254
13. Mishra A, Prasad R (2014) Preparation and Application of Perovskite Catalysts for Diesel Soot Emissions Control: An Overview. Catal Rev: Sci Engg 56(1):57–81. https://doi.org/10.1080/01614940.2014.866438
14. Mishra A, Prasad R (2015) Development of highly efficient double substituted perovskite catalysts for abatement of diesel soot emissions. Clean Techn Environ Policy 17:2337–2347. https://doi.org/10.1007/s10098-015-0976-z
15. Mishra A, Prasad R (2017) Catalysis and kinetics of diesel soot oxidation over nano-size perovskite catalyst. Clean Techn Environ Policy 19:2405–2416. https://doi.org/10.1007/s10098-017-1428-8
16. Pal DB, Singh P, Mishra PK (2017) Composite ceria nanofiber with different copper loading using electrospinning method. J Alloys Compounds 694:10–16. https://doi.org/10.1016/j.jallcom.2016.09.301

17. Shan X, Sun D, Liu H, Wang X, Yan X (2011) Fabrication of Cu-doped cerium oxide nanofibers via electrospinning for preferential CO oxidation. Catal Commun 12(6):514–518. https://doi.org/10.1016/j.catcom.2010.11.021
18. Si R, Raitano J, Yi N, Zhang LH, Chan SW, Stephanopoulos MF (2012) Structure sensitivity of the low-temperature water-gas shift reaction on Cu-CeO_2 catalysts. Catal Today 180:68–80. https://doi.org/10.1016/j.cattod.2011.09.008
19. Tang CJ, Sun JF, Yao XJ, Cao Y, Liu LC, Ge CY, Gao F, Dong L (2014) Efficient fabrication of active CuO-CeO_2/SBA-15 catalysts for preferential oxidation of CO by solid state impregnation. Appl Catal B 146:201–212. https://doi.org/10.1016/j.apcatb.2013.05.060
20. Tang H, Sun H, Chen D, Jiao X (2012) Fabrication of Pt/CeO_2 nanofibers for use in water-gas shift reaction. Mater Lett 77:7–9. https://doi.org/10.1016/j.matlet.2012.02.122
21. Wang DY, Kang YJ, Doan-Nguyen V, Chen J, Kungas R, Wieder NL, Bakhmutsky K, Gorte RJ, Murray CB (2011) Synthesis and Oxygen Storage Capacity of Two-Dimensional Ceria Nanocrystals. Angew Chem Int Ed 50:4378–4381. https://doi.org/10.1002/anie.201101043

Figures

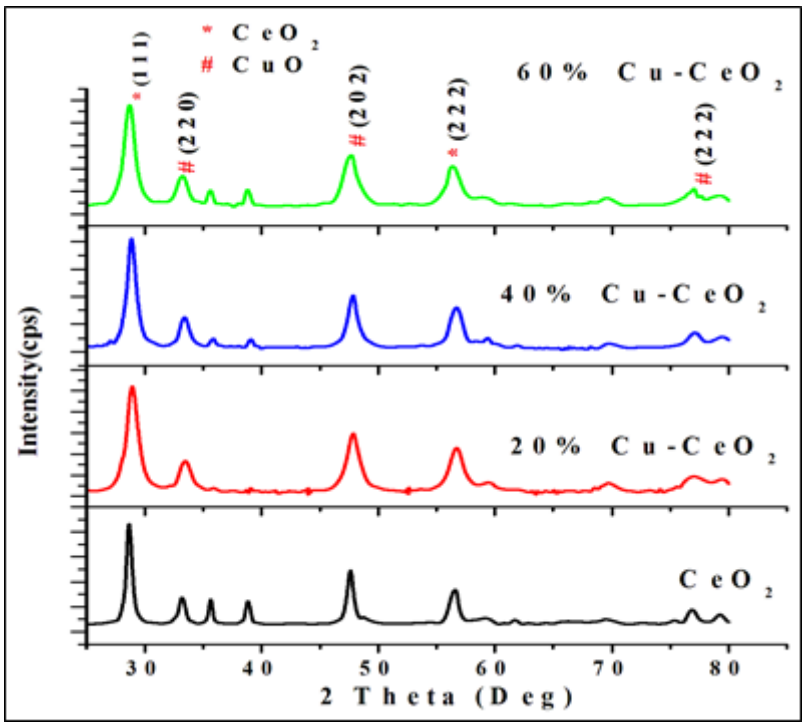

Figure 1

XRD patterns of pure and Cu loaded Ceria nanofibers.

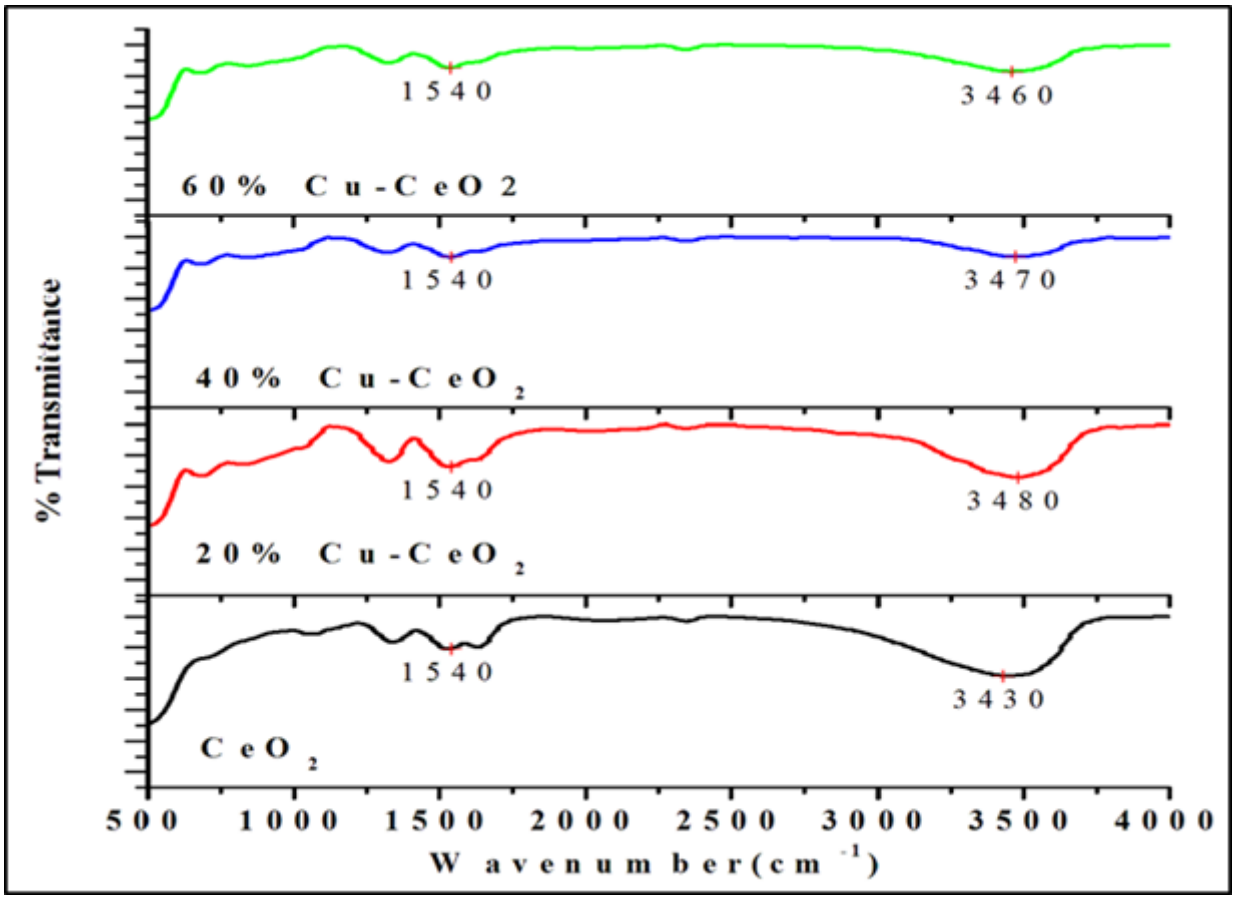

Figure 2

FTIR spectra of nanofibers pure and Cu loaded.

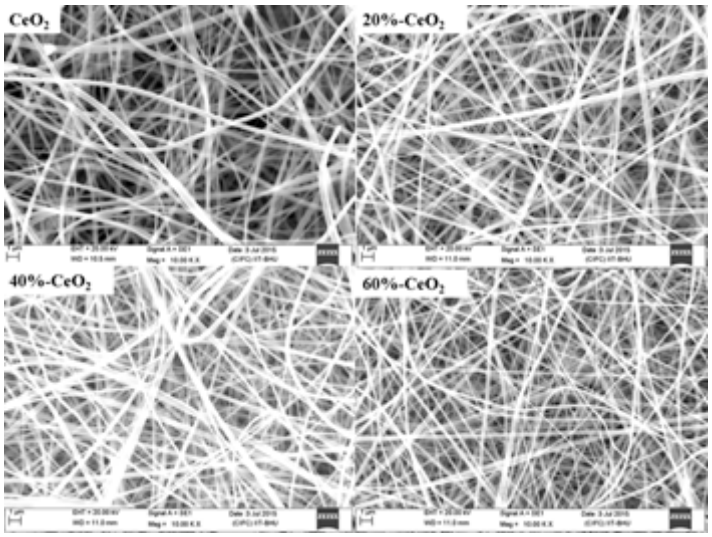

Figure 3

SEM Images of pure and Cu loaded ceria nanofibers.

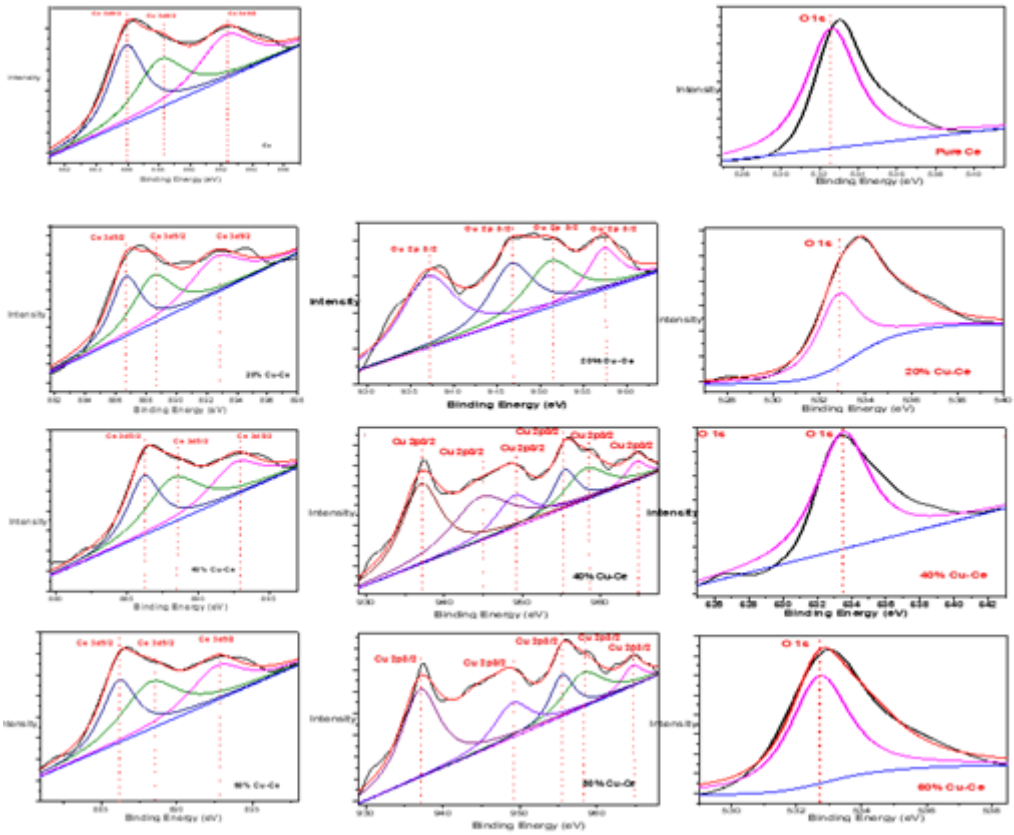

Figure 4

XPS spectra of ceria nanofibers pure and Cu loaded.

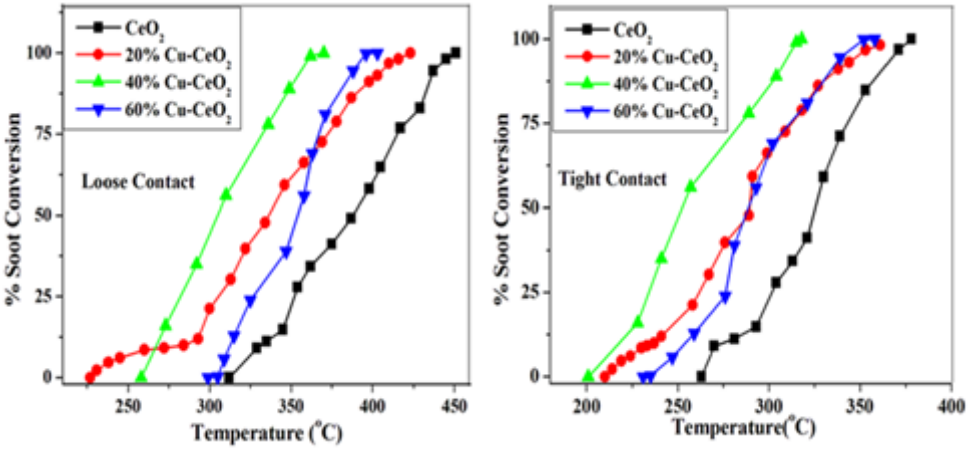

Figure 5

Performance of the Pure and Cu-Supported Ceria nanofiber catalysts for Diesel Soot Oxidation in Loose and Tight contact conditions

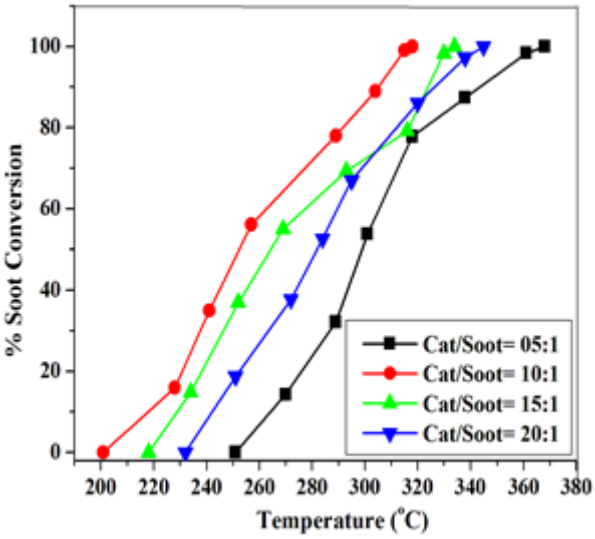

Figure 6

Characteristic light off temperature for soot oxidation over 40% Cu-CeO2 (with different Catalyst/soot ratio)

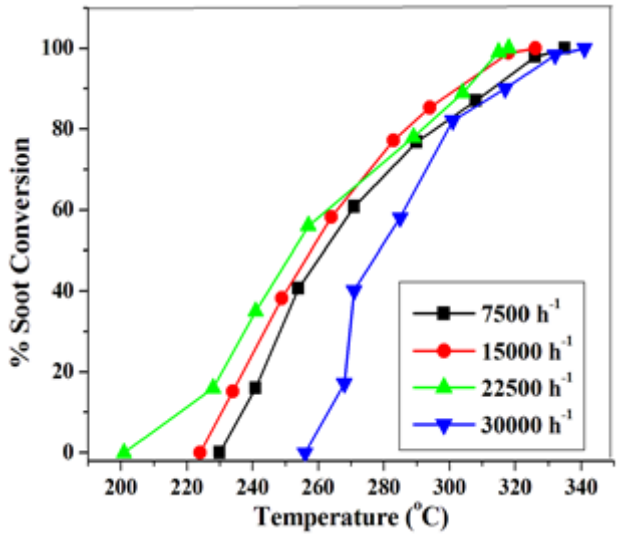

Figure 7

Effect of Gas Hourly space Velocity on soot oxidation, by 40% Cu-CeO2, (Catalyst/Soot: 10/1)

Supplementary Files

This is a list of supplementary files associated with this preprint. Click to download.

- graphicalabstract.pptx